



Spatial and temporal distribution of *Trichodesmium* blooms in the world's oceans

Toby K. Westberry^{1,2} and David A. Siegel¹

Received 16 December 2005; revised 21 July 2006; accepted 8 August 2006; published 15 December 2006.

[1] Nitrogen fixing organisms, such as the cyanobacterium *Trichodesmium*, directly affect the oceanic nutrient inventory through the addition of new nitrogen to the ocean ecosystem and therefore have an important role in the strength and functioning of the biological carbon pump. Nonetheless, little is known about the distribution of *Trichodesmium* beyond limited shipboard observations. Even less is known about the occurrence and characteristics of very intense, transient blooms of this organism that have been observed historically throughout the world oceans. A new method for discriminating the occurrence of blooms from satellite ocean color data is used here to make the first global maps of *Trichodesmium* bloom occurrence and to examine their spatial and temporal distribution. As expected, *Trichodesmium* blooms are rare, occurring <5–10% of the time over most of the tropical and subtropical oceans for the time period examined (1998–2003). Areas of greatest persistence are found in the eastern tropical Pacific and the Arabian Sea, and reach recurrence levels of >30%. Many of the retrieved patterns are consistent with previously reported blooms, though differences exist. A strong seasonal cycle is observed in the Indian Ocean, probably related to monsoonal forcing, with weaker seasonal changes elsewhere. Estimated global nitrogen fixation rates by *Trichodesmium* blooms is ~ 42 Tg N yr⁻¹ which is biogeochemically significant on regional and global scales. Further, an estimate of the rate of *Trichodesmium* nitrogen fixation under nonbloom conditions is an additional ~ 20 Tg N yr⁻¹ suggesting that *Trichodesmium* is likely the dominant organism in the global ocean new nitrogen budget.

Citation: Westberry, T. K., and D. A. Siegel (2006), Spatial and temporal distribution of *Trichodesmium* blooms in the world's oceans, *Global Biogeochem. Cycles*, 20, GB4016, doi:10.1029/2005GB002673.

1. Introduction

[2] *Trichodesmium* is a photosynthetic, nitrogen (N) fixing cyanobacterium widely distributed throughout the tropics and subtropics of the world ocean [Capone *et al.*, 1997]. It plays a key role in the oceanic N cycle through its conversion of dissolved gaseous N (N₂) to combined nitrogen. Estimated rates of N₂ fixation have steadily increased over time as more is learned about the extent and intensity of their distribution as well as the diversity of N₂ fixing genera in the ocean [Carpenter and Capone, 1992; Carpenter and Romans, 1991; Capone *et al.*, 1997; Zehr *et al.*, 2001; Montoya *et al.*, 2004]. Accordingly, the processes of N₂ fixation and its corollary, denitrification, have come to dominate the sources and sinks of N in the ocean and largely determine the size of the overall N reservoir [Codispoti *et al.*, 2001]. In turn, the rate at which ocean

biology sequesters carbon, referred to as the “biological pump,” relies on the oceanic nutrient inventory and the rates which control it [McElroy, 1983; Brandes and Devol, 2002]. This has led to hypotheses which relate changes in the nutrient supply rate and the strength of the biological pump to carbon dioxide (CO₂) cycling in the atmosphere/ocean system [Falkowski, 1997; Broecker and Henderson, 1998; Michaels *et al.*, 2001]. At present, it is not clear whether recent estimates of N₂ fixation and denitrification are balanced or imply a deficit of N in the ocean [Gruber and Sarmiento, 1997; Codispoti *et al.*, 2001].

[3] Regional and global estimates of N₂ fixation rates have a large degree of uncertainty which is likely caused by methodological reasons. Areal estimates of N₂ fixation are often scaled up on the basis of point measurements of N₂ fixation [i.e., Capone *et al.*, 2005] and spatial integration scales are not well defined and often differ from study to study (as pointed out by Hansell *et al.* [2004]). Further, these rates generally do not include contributions due to infrequent, yet large blooms of *Trichodesmium*, owing to the lack of knowledge about their distribution in space and time. Observations reported in the literature document extremely extensive and intense blooms in many parts of the ocean [Carpenter, 1983; Capone and Carpenter, 1992, and

¹Institute for Computational Earth System Science, University of California, Santa Barbara, California, USA.

²Now at Department of Botany and Plant Pathology, Oregon State University, Corvallis, Oregon, USA.

references therein], but no comprehensive descriptive or quantitative assessment of the distribution of these blooms has been made to date. Geochemical estimates of net N_2 fixation provide one way of accounting for this shortcoming, but impart their own biases [Michaels *et al.*, 1996; Montoya *et al.*, 1996; Carpenter *et al.*, 1997; Gruber and Sarmiento, 1997; Karl *et al.*, 1997]. Recent numerical modeling efforts explicitly including *Trichodesmium* N_2 fixation provide another approach for estimating areal rates and biomass, but are sensitive to details of model parameterization [Doney, 1999; Hood *et al.*, 2001, 2004; Moore *et al.*, 2002]. Divergence in each of these approach's results is not unexpected owing to the extreme differences in the methods applied.

[4] Satellite remote sensing of *Trichodesmium* provides another approach that falls somewhere between the methods described above. Indirect approaches have yielded encouraging results consistent with observations and emphasize the importance of oceanic N fixation [Coles *et al.*, 2004]. Early efforts at directly parameterizing *Trichodesmium* bio-optics worked for regional studies [e.g., Dupouy, 1992; Subramaniam *et al.*, 1999, 2002], but were not appropriate for global scales. Westberry *et al.* [2005] recently described a robust method for mapping the occurrence of *Trichodesmium* blooms that was independently validated with a globally representative data set (see section 2.2). Here this method is applied to describe the spatiotemporal distribution of *Trichodesmium* blooms in the tropical and subtropical oceans. Their occurrence and persistence is compared to previous observations of *Trichodesmium* blooms. The relationship between bulk chlorophyll (Chl *a*) and *Trichodesmium* blooms is investigated and their effect on the bio-optical assumption is discussed. Lastly, the contribution that *Trichodesmium* blooms make to global N_2 fixation rates is estimated using physiological values taken from the literature.

2. Methods

2.1. Data Sources

[5] Ocean color imagery was provided by the Sea-viewing Wide Field of view Sensor (SeaWiFS). For the global analyses, 8-day Level-3 binned Global Area Coverage (GAC) composites for the time period January 1998 through December 2003 were used. The native spatial resolution of these files is ~ 9 km at the equator, resulting in a grid size of 2096×4320 . The data have been regridded to $1/4^\circ$ (~ 27 km) spatial resolution and only data between $45^\circ N$ and $45^\circ S$ are used. Normalized water leaving radiances were extracted at 5 wave bands in the visible (412, 443, 490, 510, and 555 nm) and converted to remote sensing reflectance, $R_{rs}(0^-, \lambda)$, just below the air-water interface. Derived atmospheric correction parameters were also extracted for later use in determining atmospheric contamination; ε_{78} , the ratio of aerosol radiances in the short and long wavelengths (SeaWiFS band 7 and band 8), and A_{510} , the Angstrom coefficient at 510 nm. In addition, global fields of sea surface temperature (SST) were obtained from the Advanced Very High Resolution Radiometer (AVHRR) Pathfinder project (<http://podaac-www.jpl.nasa.gov/>) for the

same time periods. These data were also binned and interpolated to the same 8-day, $1/4^\circ$ domain as the SeaWiFS data.

2.2. Model Implementation

[6] The SeaWiFS $R_{rs}(0^-, \lambda)$ were subsequently used as input to the model of Westberry *et al.* [2005] to create corresponding maps of *Trichodesmium* bloom occurrence. Briefly, the model provides an index for the presence of *Trichodesmium* biomass above a threshold value of 3200 trichomes L^{-1} (equivalent to 0.8 mg/m^3 *Trichodesmium*-specific Chl *a* found using average values of 200 trichomes per colony and 50 ng Chl *a* per colony [Carpenter, 1983; Subramaniam *et al.*, 2002]), allowing for a “presence” or “absence” bloom designation. The robustness of this “bloom” estimate has been independently validated using both in situ and satellite observations of $R_{rs}(0^-, \lambda)$ and *Trichodesmium* abundance [Westberry *et al.*, 2005]. In the in situ model development data set, 92% of observed bloom values (>3200 trichomes L^{-1}) were correctly identified and 16% of nonbloom observations were falsely identified as blooms. Model performance in the independent satellite-in situ validation data set correctly described 76% of bloom observations and 29% false positive bloom retrievals. Given the small size of the model development and validation data sets, no consistent pattern in the location or timing of these “false blooms” is found. Further details describing model performance and validation is given by Westberry *et al.* [2005].

[7] The resulting *Trichodesmium* bloom occurrence maps have undergone a series of image processing steps. A morphological erosion filter was employed to eliminate single bloom pixels surrounded by nonbloom retrievals [e.g., Brown and Yoder, 1994]. The reasoning is that single isolated bloom pixels amid nonbloom pixels are likely to be spurious or false positive retrievals. Further, a morphological closing operator was applied to “smooth” the features by filling in small holes using a disk of radius equal to one pixel as the structuring element [Soille, 2003]. A series of masks were also applied to the blooms maps to exclude regions of uncertain quality. Pixels with $SST < 23.5C$ were neglected by evaluation of AVHRR SST at each location. Additionally, pixels with suspect atmospheric correction were also discarded. This was done by eliminating pixels where values of $\varepsilon_{78} > 1.1$ and/or $A_{510} > 0.5$. These values are upper bounds for a common maritime aerosol atmosphere (Bryan Franz, personal communication, 2005). As a final processing step, a depth mask was applied to neglect retrievals in shallow water (<100 meters) which are more difficult to interpret owing to complex optical properties of the coastal ocean and near-coastal atmospheric contamination.

[8] The overall effect of the masking procedures is small. While the combined masks eliminate positive *Trichodesmium* bloom retrievals, the overall pattern remains unchanged. Table 1 shows the extent of the masks and of changing those masks for the tropical latitudes where most blooms are found ($20^\circ S$ to $20^\circ N$). The SST mask is the most significant, eliminating ~ 6 –13% of retrieved bloom pixels in this region. If we consider higher latitudes, the SST mask

Table 1. Percentage of Positively Identified Bloom Pixels (Within 20°S–20°N) Masked by Various Procedures by Season^a

	SST = 21°	SST = 23.5°	SST = 25°	Depth Mask	Atm. Corr. Mask
Spring	3.2 ± 1.6	6.1 ± 2.0	11.5 ± 2.5	4.1 ± 0.6	9.6 ± 2.6
Summer	5.3 ± 1.2	12.2 ± 3.6	25.7 ± 6.5	4.1 ± 0.6	5.0 ± 2.2
Fall	6.8 ± 1.8	13.9 ± 3.2	24.5 ± 5.1	4.0 ± 0.5	9.3 ± 3.9
Winter	4.0 ± 1.1	10.4 ± 4.1	21.6 ± 6.1	3.6 ± 0.8	7.7 ± 2.6

^aAlso shown are results for changing SST thresholds (23.5°C is criterion used in this paper). Depth mask corresponds to water depths <100 m; atmospheric contamination mask is described in text.

excludes a much higher percentage of bloom identified pixels (not shown), particularly in the high latitudes in the Southern Hemisphere, where it is certain *Trichodesmium* cannot grow owing to physiological constraints (not shown) [Capone *et al.*, 1997; Karl *et al.*, 2002]. Both the depth mask and the atmospheric correction mask each eliminate ~4–10% of additional bloom pixels. There is very little seasonality in the total fraction of pixels masked (Table 1). On average, approximately $23 \pm 3\%$ of classified bloom pixels were masked owing to the SST, atmospheric, and depth masks. In practice, most of these outliers were overlapping such that they met more than one of the criteria for masking.

3. Results

[9] *Trichodesmium* bloom occurrence maps were created for January 1998 to December 2003. The average percent time when a *Trichodesmium* bloom occurs can be calculated by sequentially summing the occurrence maps and dividing by the total number of clear sky observations. However, to account for biases due to clouds, this ratio is further scaled to the frequency of clear skies at each particular location (Figure 1). In general, blooms are rare, occurring less than 5% of the time for most locations. Maximum values approach 35% and are found in the northern Arabian Sea and in the eastern Pacific centered on 10°S and 120°W indicating that bloom quantities of *Trichodesmium* populate

these regions approximately one third of the time. Other areas of persistent bloom occurrence (~10% of the time) are the Caribbean, the southern Indian Ocean, the eastern tropical Atlantic and the eastern tropical north Pacific. The rest of the ocean sees *Trichodesmium* blooms infrequently with ~70% of the tropical and subtropical surface ocean (45°S–45°N) experiencing blooms less than 5% of the time (Figure 2). The cumulative probability distribution function also indicates 90% of the ocean between 45°S and 45°N experiences blooms less than 10% of the time while 30% of the ocean examined never sees a *Trichodesmium* bloom as defined here.

[10] Over broad regions, seasonal patterns are evident in bloom occurrence that appear out of phase from one ocean basin to another (Figures 3a–3d). The Indian Ocean, whose atmospheric and oceanic responses are dominated by monsoonal flow, shows dramatic changes through the year. Maxima in persistence are observed during the Fall (September–November) in the Arabian Sea and along the western boundary near Oman and Somalia. These are the highest values found anywhere and show that blooms are observed ~45% of the time during these months. A strong bloom persistence signal is also found in the winter, and in fact, the most widespread and persistent blooms in the Arabian Sea straddle the seasons (October, November, December (not shown)). This time period corresponds to the fall intermonsoon period and onset of the northeast winter monsoon (not upwelling favorable). It is possible that the decrease in upwelling during this period creates a N-starved environment. Satellite coverage during the summer is problematic owing to dust and clouds and it is difficult to diagnose bloom occurrence during this period [e.g., Banzon *et al.*, 2004].

[11] In the Pacific (Figures 3a–3d), blooms are present throughout the year south of the equator growing to $\sim 5.4 \times 10^6$ km² during the boreal winter (December–February) and they are about half this size during the fall (September–November). Maximum persistence is >40% in very small areas and are ~20–30% over large areas of this region during the winter. Also in the eastern tropical Pacific, the

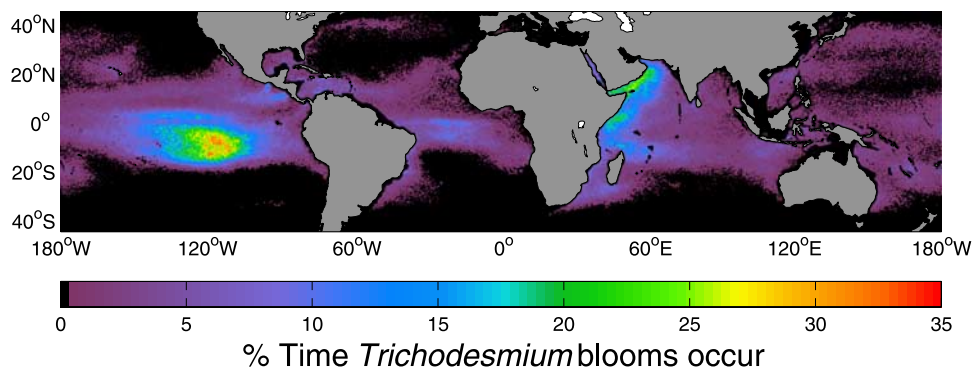


Figure 1. Percent of time *Trichodesmium* blooms are present (persistence) as estimated from SeaWiFS. The percentage of time is calculated at each pixel as the fraction of clear-sky observations which are identified as *Trichodesmium* blooms between January 1998 and December 2003, scaled to the frequency of clear-sky occurrences during that period. Bloom fields calculated at a spatial resolution of 1/4° (~27 km) using 8-day SeaWiFS reflectance data.

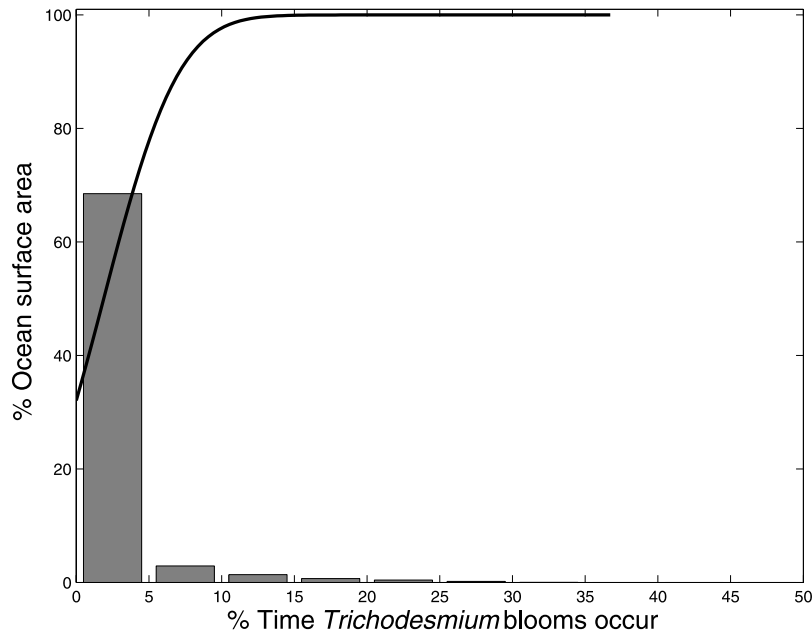


Figure 2. Histogram of *Trichodesmium* bloom occurrence globally. Values expressed as percentage of ocean surface (between 45°S and 45°N) which supports a given level of bloom persistence. Also shown is cumulative distribution curve (solid line).

bloom area off of Central America exhibits a strong seasonality, virtually disappearing during the summer. During the winter, *Trichodesmium* blooms occur up to ~25% of the time. Bloom features in this area do not correspond exactly with the strong Chl *a* signal in the Gulf of Tehuantepec or the Costa Rica Dome [Fiedler, 2002; Xie *et al.*, 2005]. *Trichodesmium* bloom occurrence is ~10% of the time around the Costa Rica Dome and appears on the flanks of the Chl *a* signal off of southern Mexico, except during the winter when much of the Chl *a* signal is coincident with retrieved *Trichodesmium* blooms (not shown).

[12] The Atlantic Ocean exhibits comparatively fewer blooms (persistence <20%) and a correspondingly smaller degree of seasonality. In the summer and fall, *Trichodesmium* blooms are found in the equatorial Atlantic as well as the Gulf Stream and features in the Caribbean and western equatorial Atlantic, are strongest in the winter and spring, but still only exhibit blooms <20% of the time (Figure 3). Features along the African coast are more transient and ill-defined possibly owing to dust contamination issues in the satellite imagery.

[13] Interannual variability in *Trichodesmium* bloom persistence exists in each ocean basin as well (Figure 4). By summing the *Trichodesmium* bloom retrievals zonally in 2° bands, the areal percent coverage of *Trichodesmium* blooms within each 2° band can be expressed. Figures 4a–4c shows this quantity throughout the first 6 years of the SeaWiFS mission in each ocean basin. The Pacific Ocean exhibits a large degree of interannual variability with maxima in intensity and zonal extent of blooms in 2000. The years 2001–2002 also have periods of widespread *Trichodesmium* blooms, while blooms in 1998–1999 and 2003 occur less frequently over smaller zonal scales. Most of the blooms in the Pacific occur south of the equator. Also

plotted in Figure 4a is the monthly averaged Southern Oscillation Index (SOI) which gives a measure of inter-annual climate variability in the Pacific. There is a rough correspondence between relative changes in the amount of *Trichodesmium* blooms and the strength of the SOI, where positive excursions in the SOI correspond to greater areal extent of *Trichodesmium* blooms. This is especially evident in the beginning of the record, which is a strong El Niño–La Niña transition period. Other large-scale changes in the surface ocean biota have been well documented during this period [e.g., Behrenfeld *et al.*, 2001]. However, the ENSO cycle has been more stable since this time and the levels of corresponding variability in bloom occurrence are also more stable. If the areal coverage is integrated meridionally, the correlation coefficient with the SOI is 0.25 (*r* value; significant at the 95% c.l.) where high SOI corresponds to higher *Trichodesmium* bloom occurrence.

[14] The Atlantic Ocean shows the least extensive or persistent *Trichodesmium* bloom occurrences (Figure 4b). Maxima in areal bloom coverage are also south of the equator but cover only ~10% of a given zonal band. Variability in both latitude and time is more uniform than other ocean basins. Overlaid on the Atlantic pattern (Figure 4b) is the monthly averaged North Atlantic Oscillation (NAO) index which shows no obvious correspondence between the NAO and bloom coverage. Integrating bloom coverage meridionally as before yields a weak correlation with the NAO (*r* = 0.11, not significant at 95% c.l.). It seems likely that bloom formation is responding to more local forcing (i.e., PO₄ input from the Amazon or aeolian dust deposition from North Africa).

[15] Blooms in the Indian Ocean appear regularly during the fall and winter, but with a large degree of interannual variability embedded in the seasonal pattern (Figure 4c). As

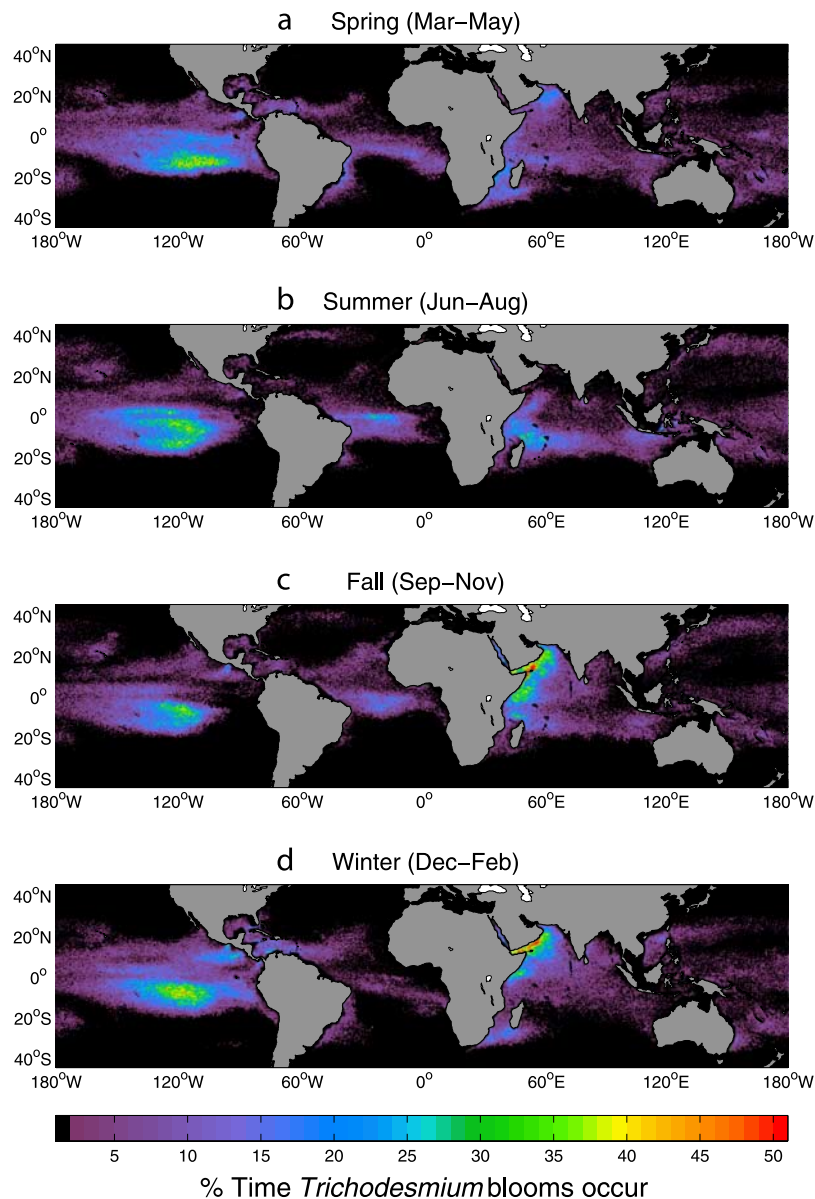


Figure 3. Percent of time *Trichodesmium* blooms are present seasonally (persistence). Calculated as in Figure 1 but for particular months, (a) March–May, (b) June–August, (c) September–November, and (d) December–February.

in the global persistence map (Figure 1), most of this ocean sees very little coverage by *Trichodesmium* blooms, on the order of <5% of each 2° band in this case. Latitudes where blooms frequently occur (>30% of the time) correspond to the northern Arabian Sea and to a lesser extent around 18°S, on the western margin of the Indian ocean near Madagascar (Figure 1). These signals are out of phase with one another with maxima north of the equator closer to winter, while the maxima in the southern Indian Ocean appear in the Northern Hemisphere summer (Figure 4c). The Arabian Sea pattern is also out of phase with the evolution of the Chl *a* pattern as Chl *a* concentrations reach their peak in July–August for this region [Banzon *et al.*, 2004]. Also plotted in Figure 4c is another index of interannual variability, the Dipole Mode Index (DMI) [Saji *et al.*, 1999; Saji and

Yamagata, 2002]. The DMI is a measure of the east-west SST gradient across the Indian Ocean and has been related to interannual variability in monsoon strength and other aperiodic phenomena such as ENSO. This index is not significantly correlated with the zonally integrated bloom abundance ($r < 0.1$).

4. Discussion

4.1. Comparison to Previous Assessments of *Trichodesmium* Bloom Occurrence

[16] The global, satellite observation-derived maps of *Trichodesmium* bloom occurrence presented here are the first of their kind. It is therefore important to compare the present patterns of *Trichodesmium* bloom occurrence with

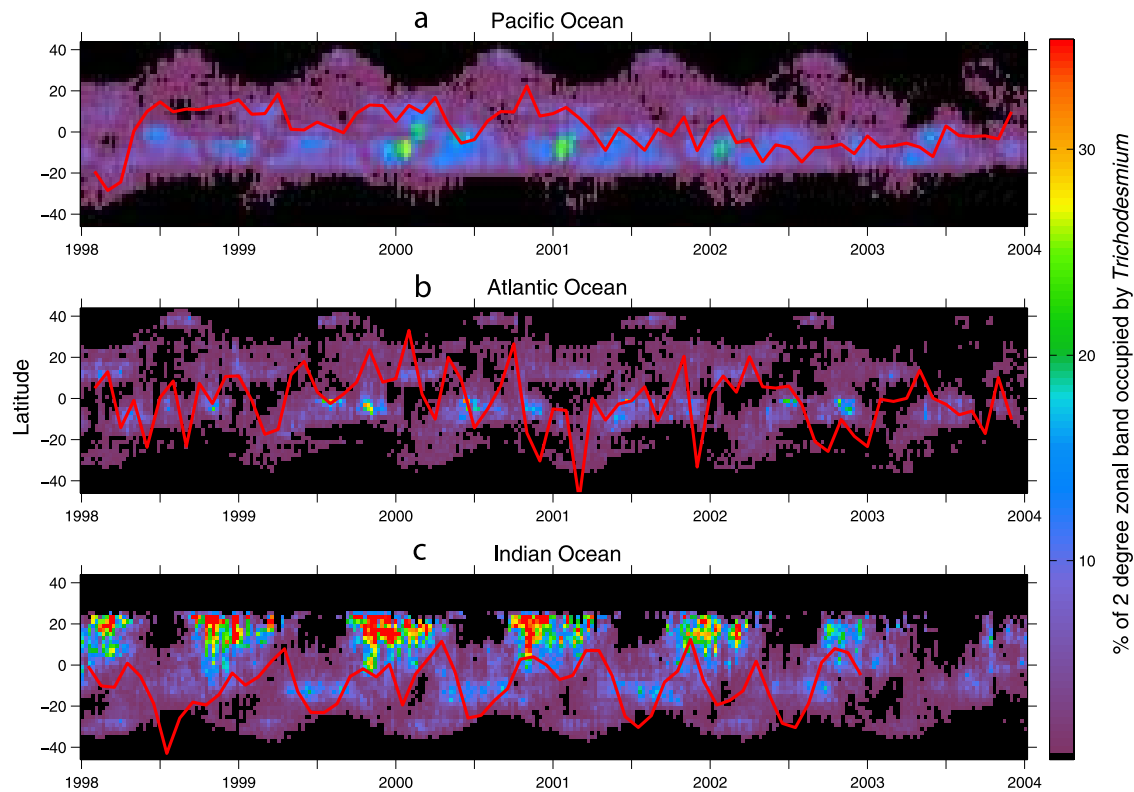


Figure 4. Fraction (expressed as percentage) of each zonally averaged 2° band covered by *Trichodesmium* blooms within each ocean basin, (a) Pacific, (b) Atlantic, and (c) Indian. Also shown as solid lines are the monthly averaged composite SOI, NAO, and DMI for the Pacific, Atlantic, and Indian Oceans, respectively (see text for description of climate indices). The SOI, NAO, and DMI have been scaled to fit within the axis provided.

previously published accounts. This is not a straight forward task as field measurements of *Trichodesmium* bloom occurrence are single point observations and are not areal estimates of biomass. Hence small-scale variations of abundance in horizontal distance or with depth can make assays of *Trichodesmium* abundance highly uncertain [Subramaniam *et al.*, 2002]. Further, observations are often

made using different techniques making their comparisons difficult. Owing to its rarity, relatively few observations of *Trichodesmium* blooms have been published making the elucidation of general patterns and trends difficult.

[17] The bio-optical approach used here to map *Trichodesmium* bloom occurrence has its limitations as well [Westberry *et al.*, 2005]. Algorithm validation using an

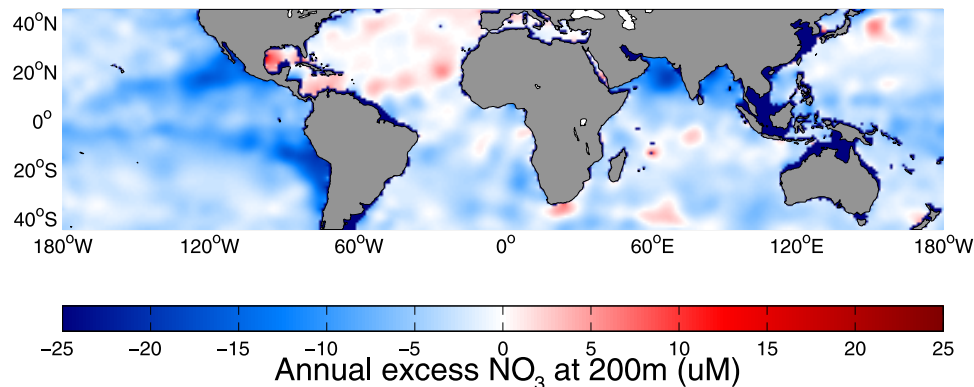


Figure 5. Mean annual excess nitrate at 200 m. Data are taken from the World Ocean Atlas 2001 [Conkright *et al.*, 2002] and are climatological mean values at 1° resolution. Excess nitrate calculated as $[\text{NO}_3] - 16 \times [\text{PO}_4]$.

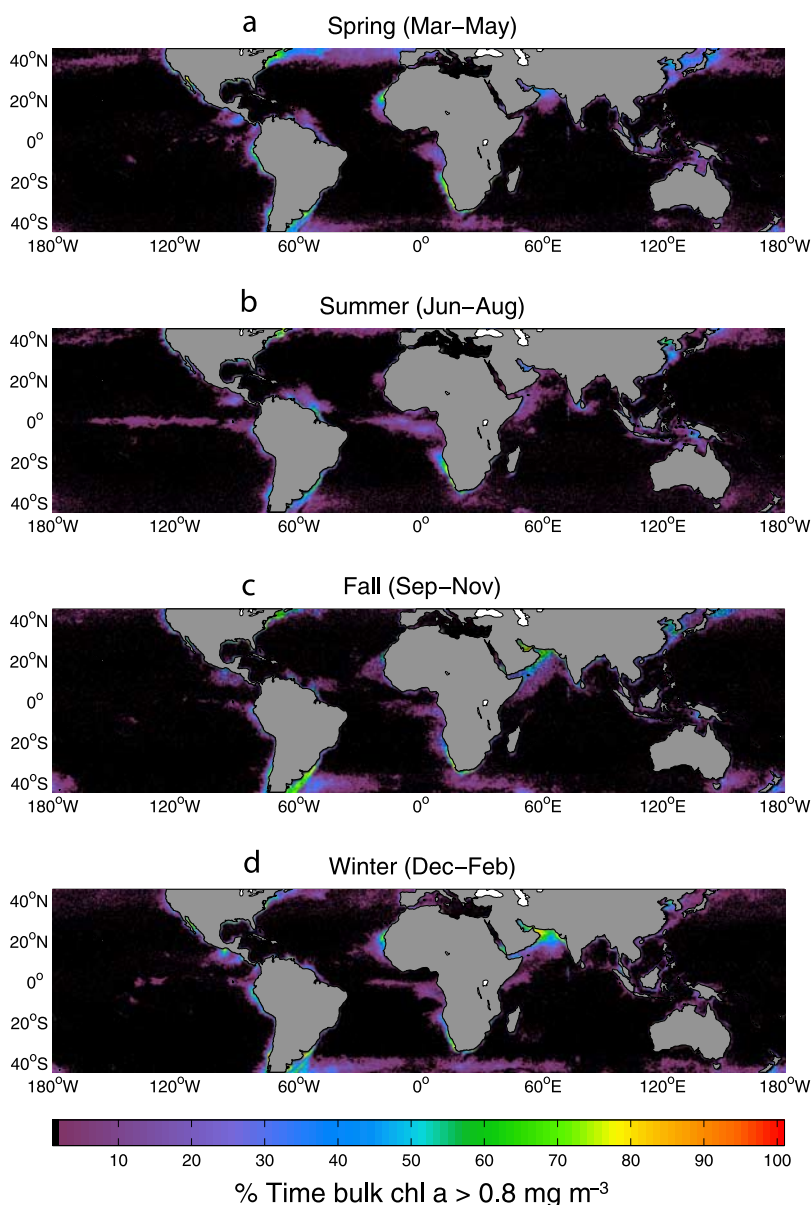


Figure 6. Percent of time which SeaWiFS Chl *a* > 0.8 mg m⁻³ seasonally for (a) March–May, (b) June–August, (c) September–November, and (d) December–February. The percentage of time is calculated at each pixel as described in Figure 1. Values calculated at a spatial resolution of 1/4 ° (~27 km) using 8-day Chl *a* data.

independent data set resulted in false positive bloom retrievals ~29% of the time. This can be significant and so the image processing undertaken here was meant to minimize these retrievals (i.e., SST mask, atmospheric correction mask, removal of single bloom pixels, etc). In addition, the scale of the satellite measurements (both spatial and temporal) can affect the retrieved patterns by assuming uniformity over a pixel and the duration of the measurement (e.g., 8 days). For example, a bloom which covers just over half of a pixel and lasts for ~5 days, may be enough to be identified as a *Trichodesmium* bloom. Thus the persistence values presented here can be viewed as an upper bound. Previous efforts to synthesize *Trichodesmium*

distributions provide coarse descriptions of its distribution [e.g., Carpenter, 1983; Carpenter and Capone, 1992; Karl *et al.*, 2002; Capone *et al.*, 2005]. The emphasis of these reviews has been primarily on subbloom densities of *Trichodesmium* simply because they are observed more often. However, it is valid to compare against these representations and point out similarities and differences under the assumption that blooms will arise in regions where *Trichodesmium* abundances are found in general. Carpenter [1983] pooled available literature reports of *Trichodesmium* occurrence in the world ocean and synthesized them into seasonal maps of abundance (see his Figures 4–7). Broad-sweeping assumptions needed to

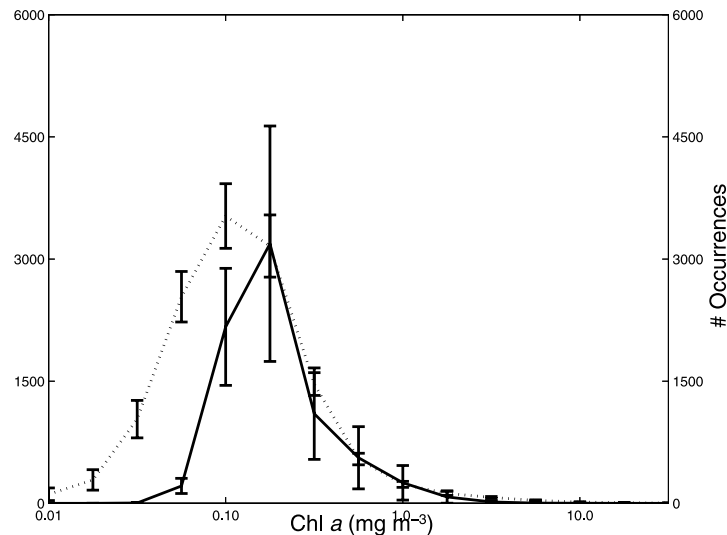


Figure 7. Mean ($\pm 1\sigma$) SeaWiFS Chl *a* distributions for pixels classified as *Trichodesmium* blooms (solid line) and those that are not (dotted line). For each 8-day bloom image, a histogram of each condition was generated and the mean ($\pm 1\sigma$) for all 8-day images from 1998–2003 are shown ($N = 276$). Frequency of nonbloom observations have been scaled to fit axis by 1/20.

be made as each global seasonal composite was constructed from 15–20 individual observations. One notable feature in that analysis is the presence of *Trichodesmium* in the western boundary currents (Gulf Stream and Kuroshio Current system) during the summer and fall and its marked absence during the winter and spring. Figure 3 shows a similar pattern in the SeaWiFS retrievals of *Trichodesmium* bloom occurrence, especially in the eastern reaching extensions across the North Atlantic and western North Pacific. Carpenter [1983] also showed elevated abundances of *Trichodesmium* in the central North Pacific during the same time period, summer and fall (June–November). Again, this pattern is observed in the SeaWiFS bloom estimates, although bloom occurrence still amounts to a small percentage of the total time (Figure 3). Carpenter [1983] also showed fairly persistent levels of *Trichodesmium* ($\sim > 10^5$ trichomes m^{-3}) throughout the northern Indian Ocean in the fall and winter. Still higher values ($> 10^6$ trichomes m^{-3}) were noted along the eastern margin of the African continent during the winter, as well. Both of these observations are broadly consistent with the patterns seen in Figure 3, which show strong seasonal appearance in this region during the fall and winter months.

[18] Carpenter and Capone [1992] compiled several dozens of reported *Trichodesmium* blooms and identified areas likely to experience persistent blooms. Those areas were the Arabian Sea, the west coast of Africa, the northwest coast of Australia, the Caribbean and Gulf of Mexico, and the southwest Pacific near New Caledonia and Vanuatu. The maps in Figure 1 and Figure 3 share many of these characteristics. The shallow seas north of Australia do not show up in this analysis owing to the depth mask used in satellite data processing which is unfortunate as there are repeated observations of intense blooms in this area [Carpenter and Capone, 1992]. Another area which does not exhibit persistent blooms in the analyses presented here

but noted by Carpenter and Capone [1992] is the southwest Pacific Ocean ($20^\circ S$, $180^\circ E$). Extremely large blooms have been reported in this area [Dupouy, 1992], however, their frequency is not well documented in situ and are observed infrequently using the satellite-based maps presented here.

[19] In addition to direct shipboard observations, the satellite-based maps of *Trichodesmium* bloom occurrence can be compared with geochemical inferences of net N_2 fixation [e.g., Michaels et al., 1996; Gruber and Sarmiento, 1997; Deutsch et al., 2001; Hansell et al., 2004]. Geochemical estimates are integrative measurements that reflect the net balance between N_2 fixation and denitrification such that, if both processes are operating equally, a geochemical signature may not be apparent. Further, the geochemical approach includes contributions from all diazotrophs, not just *Trichodesmium* [e.g., Zehr et al., 2001; Capone et al., 2005].

[20] As a first-order proxy for geochemical N_2 fixation we calculate excess nitrate concentrations from nitrate and phosphate data taken from the World Ocean Data Atlas 2001 [Conkright et al., 2002]. This is a simplified version of the N^* parameter [Michaels et al., 1996; Gruber and Sarmiento, 1997] and is defined here as the difference between the nitrate and $16\times$ the phosphate concentration objectively analyzed at 200 m depth (Figure 5). Positive N^* values indicate excess nitrate relative to the Redfield ratio, presumably due to net nitrogen fixation; while negative values indicate a nitrate deficit relative to Redfield. Figure 5 shows that the North Atlantic Ocean has large regions of excess nitrogen as indicated by widespread positive N^* anomalies, suggesting widespread areas of net N_2 fixation. In contrast, the Pacific Ocean and Indian Ocean on the whole have significant nitrate deficits, indicating an excess of denitrification over N_2 fixation.

[21] Interestingly, the present satellite maps of *Trichodesmium* bloom occurrence (Figures 1 and 3) show nearly the

opposite pattern as the excess nitrate distribution (Figure 5). Regions of semipersistent *Trichodesmium* blooms, especially the eastern tropical Pacific and the northern Indian Ocean, more often than not overlay areas with neutral or large nitrate deficits, which suggest water column denitrification [Deuser, 1975; Ganeshram et al., 2000; Altabet et al., 1999]. This is opposite from that which might be expected from areas with abundant nitrogen fixers, such as blooms of *Trichodesmium*. It is possible that these regions may be good habitats for diazotrophs because the N:P ratio is driven down owing to inorganic nitrogen losses, possibly creating a nitrogen limited environment, and blooms of *Trichodesmium*. Indeed, nitrogen isotopic evidence shows that ~40% of the nitrate at 80 m depth was locally derived from N₂ fixation in the Arabian Sea, an otherwise active region of denitrification [Brandes et al., 1998]. This may also be happening in the eastern Tropical Pacific as well [Sigman et al., 2005]. Clearly, the issue of an apparent coupling between water column denitrification and N₂ fixation cannot be resolved here and detailed studies are required. The present observations of *Trichodesmium* bloom occurrence near regions of net denitrification are consistent with the right conditions (high P, low N, high light, etc.) for *Trichodesmium* populations to thrive.

[22] Last, numerical simulations of pelagic ecosystems that explicitly include *Trichodesmium* N₂ fixation or give quantitative estimates of *Trichodesmium* biomass [e.g., Hood et al., 2004; Moore et al., 2002] may be used as another measure for comparison with the satellite-retrieved patterns. Hood et al. [2004] modeled N₂ fixation for the domain spanning the tropical and subtropical Atlantic, Caribbean, and Gulf of Mexico. The authors found a springtime maximum in *Trichodesmium* biomass and N₂ fixation rates for the Gulf of Guinea and an autumn maximum in the western tropical Atlantic off Cuba and the Dominican Republic and into the Gulf of Mexico. Many of these features are consistent with the remote sensing estimates of bloom occurrence while some are not (Figure 3). The remote sensing estimates find an autumn maximum in the Gulf of Mexico although it is displaced farther north than Hood et al. [2004] and there is no large region of persistent blooms in the greater western Atlantic Ocean. There is some correspondence during the summer in the south equatorial Atlantic which shows elevated levels of *Trichodesmium* in the work of Hood et al. [2004] and higher frequency of occurrence in the remote sensing estimates also. However, the patterns shown here do not exhibit much of the activity close to the west coast of Africa. Comparison with the model output of Moore et al. [2002] also shows mixed results. The satellite retrieved bloom patterns (Figure 1) show similar features in the eastern tropical Pacific and off the African coast near Madagascar. Additionally, the blooms diagnosed in the Indian Ocean (Figure 1) are mostly in the Arabian Sea and do not extend to the Bay of Bengal as is shown by Moore et al. [2002, their Figure 11]. Again, owing to our screening process, we are unable to diagnose blooms in the shallow seas in the northwest of Australia and in the often dust-influenced west coast of Africa.

[23] In summary, the patterns of *Trichodesmium* blooms presented here share many of the features of previous

descriptions, but also have some significant differences. The most prominent difference is in the central tropical South Pacific, which is grossly undersampled by traditional shipboard measurements. To the best of our knowledge, there are no reports of *Trichodesmium* blooms for this region. The other prominent feature is the pattern in the Arabian Sea. The suggestion that *Trichodesmium* blooms could be occurring in parts of the ocean traditionally thought of as dominated by denitrification processes is novel, but is not without basis [e.g., Brandes et al., 1998; Sigman et al., 2005]. In addition, Capone et al. [1998] observed a large bloom ($\sim 2 \times 10^6$ km²) in the central Arabian Sea and speculated that they may be much more frequent and widespread than previously thought. The authors also suggested that the blooms might be an important episodic source of combined N and organic matter to fuel denitrification.

4.2. Relationship to Bulk Chlorophyll *a* Retrievals

[24] It might be expected that *Trichodesmium* blooms and blooms of other phytoplankton, as assessed using SeaWiFS Chl *a*, would be mutually exclusive because *Trichodesmium* generally grow well where other phytoplankton do not (i.e., under nitrogen limitation). However, part of the Chl *a* signal must include the contribution from *Trichodesmium*. Therefore it is not surprising that the spatial nature of the *Trichodesmium* blooms corresponds to some of the features of the Chl *a* distribution in SeaWiFS images. To contrast with seasonal patterns in *Trichodesmium* blooms (Figures 3a–3d), Figures 6a–6d show similar views of bulk phytoplankton Chl *a* retrieved from SeaWiFS. The figure shows a similar measure of persistence in bulk Chl *a* blooms; specifically the percent of time during the period examined that Chl *a* > 0.8 mg m⁻³ which is roughly equivalent to the *Trichodesmium* bloom threshold of 3200 trichomes L⁻¹. Clearly, the Chl *a* bloom occurrence patterns shown in all four seasons (Figures 6a–6d) are markedly different than those seen in Figures 3a–3d. Features are almost entirely confined to the coast and are found primarily in the productive upwelling regions. Many of the areas highlighted also show no corresponding signal in the *Trichodesmium* bloom maps (e.g., South China Sea, Benguela Current system). Maximum values of persistence in these regions are much higher than any instances found in the *Trichodesmium* bloom distributions and are easily 100% over broad coastal regions in all four seasons. Co-occurrences of *Trichodesmium* and Chl *a* bloom retrievals occur only rarely over most of the ocean. Only in the Arabian Sea do *Trichodesmium* and Chl *a* bloom retrievals overlap often (up to ~30% of the time on a seasonal basis). In general though, overlap is minimal (<10% persistence).

[25] Mean values of the SeaWiFS Chl *a* distribution ($\pm 1\sigma$) for all pixels classified as *Trichodesmium* blooms and those which are not classified as *Trichodesmium* blooms are shown in Figure 7. The distribution of Chl *a* values during non-*Trichodesmium* bloom conditions has a lower mode (~ 0.1 mg m⁻³) compared with bloom conditions. Retrieved Chl *a* values during *Trichodesmium* blooms are greater (median = 0.18 mg m⁻³) and the distribution has higher skewness (1.88) and excess kurtosis (2.13). In addition, the

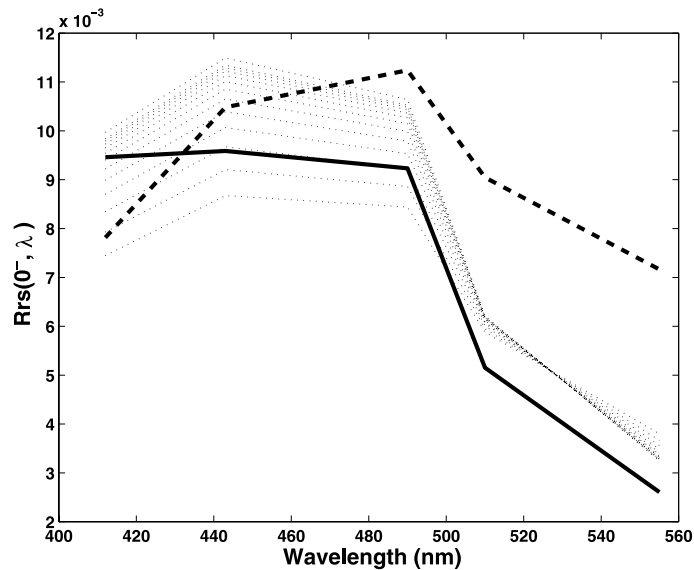


Figure 8. Spectral remote sensing reflectance, $R_{rs}(0^-, \lambda)$, for various *Trichodesmium*-specific chl *a* concentrations. Spectra are calculated using model of *Westberry et al.* [2005] with a constant background chl *a* = 0.1 mg m⁻³ and CDOM absorption = 0.02 m⁻¹. Also shown is a reference spectra (dotted line) with no *Trichodesmium* [after *Maritorea et al.*, 2002] and *Trichodesmium* bio-optical model with *Trichodesmium*-specific chl *a* = 1.0 mg m⁻³. (dashed line [Subramaniam *et al.*, 2002]).

coefficient of variation is generally much larger across the entire range of Chl *a* in the bloom classified pixels, indicating that the *Trichodesmium* fraction of total Chl *a* is much more variable.

[26] Only a small fraction of the *Trichodesmium* bloom classified pixels exhibit bulk Chl *a* retrievals greater than 0.8 mg m⁻³ (the *Trichodesmium* bloom threshold). However, this fraction relative to the total amount of occurrences is much greater in the bloom pixels than the nonbloom pixels. Nonetheless, there are numerous reasons that the bulk Chl *a* might be underestimated in the presence of *Trichodesmium*. Pigment packaging effects are large [Subramaniam *et al.*, 1999] and “secondary” packaging effects due to colony formation are also very strong [Borstad *et al.*, 1992]. Borstad *et al.* [1992] demonstrated that the absorption cross section of an average colony would be one hundred times less than that of the individual trichomes which are contained, and that a factor of 3–10 should apply for the effect of shadowing. In addition, Subramaniam *et al.* [2002] suggested this effect would underestimate the total Chl *a* by a factor of four. Therefore it is not surprising that very few of the bloom identified pixels have relatively low retrieved Chl *a* concentrations.

4.3. Contribution of *Trichodesmium* to Ocean Color Properties

[27] The effects of *Trichodesmium* on ocean color spectra (and the resulting chl *a* retrievals) can be investigated using the model of *Westberry et al.* [2005]. Run in forward mode, the *Westberry et al.* [2005] model can estimate $R_{rs}(0^-, \lambda)$ for a given background Chl *a*, colored dissolved organic matter (CDOM) absorption, and *Trichodesmium* biomass. Figure 8 shows $R_{rs}(0^-, \lambda)$ for varying amounts of

Trichodesmium biomass (0–4000 trichomes L⁻¹) and a constant background Chl *a* = 0.1 mg m⁻³ and CDOM absorption = 0.02 m⁻¹ (thin dotted lines in Figure 8). Also shown is a reference spectrum representing bulk phytoplankton from the model of *Maritorea et al.* [2002] with the same Chl *a* concentration, CDOM absorption, and particulate backscatter equivalent to Chl *a* = 0.1 mg m⁻³ (solid line in Figure 8). For the extreme range of *Trichodesmium* biomass shown there is a subtle increase in the blue to green reflectance as *Trichodesmium* biomass increases but with no real changes above 500 nm. In contrast, the $R_{rs}(0^-, \lambda)$ estimated from *Subramaniam et al.* [2002] overemphasizes *Trichodesmium* backscatter and phycoerythrin fluorescence as well as absorption by CDOM (thick dashed line in Figure 8). Both of these effects have been tempered by the optimization procedure described by *Westberry et al.* [2005] and allow the subtle distinction between *Trichodesmium* blooms and nonbloom conditions. Further, if the *Westberry et al.* [2005] modeled reflectances shown in Figure 8 are run through the operational SeaWiFS chl *a* algorithm (OC4v4 [O’Reilly *et al.*, 1998]) the Chl *a* values retrieved are underestimated by a factor of ~2x (not shown). This implies that the optical signature from *Trichodesmium* blooms is a much more subtle signal than once was believed, except, perhaps, for extremely dense surface blooms.

4.4. N₂ Fixation by *Trichodesmium* Blooms

[28] The biogeochemical impact of the bloom patterns presented here can be directly assessed by estimating the global N₂ fixation due to *Trichodesmium* blooms. The simplest approach is to apply a constant areal rate of nitrogen fixation taken from literature and extrapolate to the

Table 2. Areally Integrated *Trichodesmium* Bloom N₂ Fixation Rates in the Different Ocean Basins During Different Seasons^a

	Bloom N ₂ Fixation Rate, Tg N yr ⁻¹				Total
	Spring	Summer	Fall	Winter	
Pacific	6.9	6.9	4.5	7.1	25.4
Atlantic	1.3	1.3	1.2	0.9	4.7
Indian	2.5	2.4	3.6	3.0	11.5
Total	10.7	10.6	9.3	11.0	41.6

^aRates are reported as mean values for period 1998–2003 and are calculated using seasonal persistence fields shown in Figure 3. Values are expressed in Tg N yr⁻¹ (1 Tg = 10¹⁵ g).

total surface area covered by blooms and their observed persistence. Observations of N₂ fixation rates by *Trichodesmium* were recently summarized by Capone *et al.* [2005]. From that study, a value of 1500 μmol N m⁻² day⁻¹ is used here to represent typical values under bloom conditions. If applied to the seasonal persistence fields (Figure 3) and then summed over the seasons, the annual mean N₂ fixation rate is ~42 Tg N yr⁻¹ (Table 2). Recent geochemical estimates of total pelagic N₂ fixation are ~110 ± 40 Tg N yr⁻¹ [Gruber and Sarmiento, 1997; Codispoti *et al.*, 2001; Gruber and Sarmiento, 2002]. Thus *Trichodesmium* blooms are a significant source of fixed N to the ocean.

[29] Both the temporal and spatial pattern of the bloom N₂ fixation follow the patterns in bloom abundance. On an annual basis the largest fraction comes from the Pacific Ocean (~60%), while the least amount of *Trichodesmium*

bloom N₂ fixation arises in the Atlantic (~11%). However, it is clear from recent syntheses that some of the times, much of the diazotrophic biomass and nitrogen fixation in the Atlantic can be due to picoplanktonic diazotrophs and diatom-cyanobacterial symbioses, i.e., *Richelia* and *Hemialus*, rather than *Trichodesmium* [Carpenter *et al.*, 2004; Capone *et al.*, 2005]. The period of peak bloom N₂ fixation is different from basin to basin and never goes to zero. Pacific blooms fix the most N₂ in the winter (i.e., blooms are most widespread and persistent). The annual cycle in the Atlantic Ocean is very small with only a slight decrease in the winter months. In the Indian Ocean, the maxima correspond to the fall and winter, although there is a slow increase throughout the late summer and fall (not shown). The timing of this suggests that the rise in N₂ fixation (and bloom abundance) is not associated with the summer monsoon which brings vigorous upwelling and chl *a* biomass accumulation.

[30] Contributions from nonbloom *Trichodesmium* populations to global N₂ fixation rates can also be estimated. Using observations of *Trichodesmium* abundance compiled in Westberry *et al.* [2005] we can say something about the proportion of bloom observations to nonbloom observations. Roughly 50% of these observations can be considered negligible (<100 trichomes L⁻¹), and *Trichodesmium* abundances ranging from 100–3200 trichomes L⁻¹ represented 39% of the distribution, while bloom observations (>3200 trichomes L⁻¹) comprise the uppermost 11th percentile of this distribution (Figure 9). Assuming that the relative fraction of bloom and subbloom observations

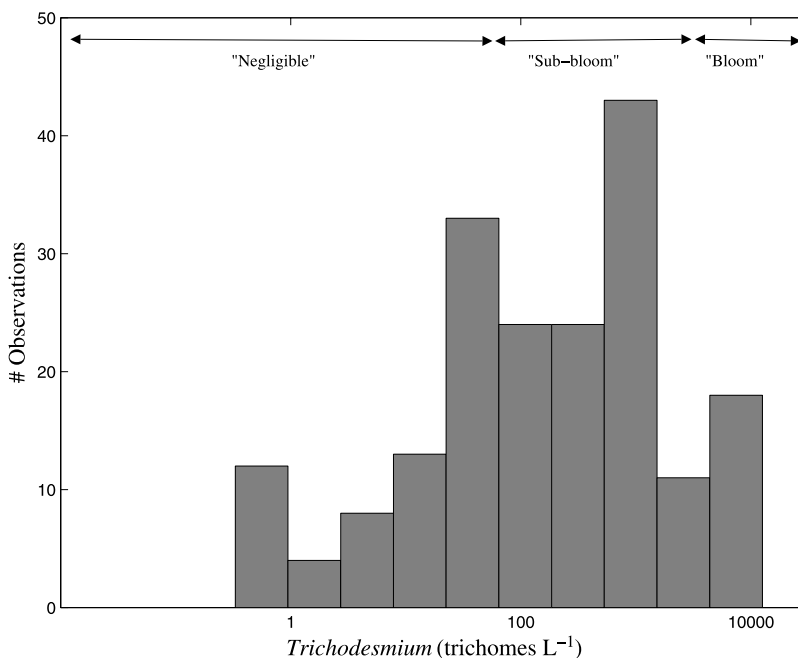


Figure 9. Histogram of in situ *Trichodesmium* abundance observations. Regions indicated are designated as negligible, subbloom, and bloom abundances and correspond to *Trichodesmium* biomass <100 trichomes L⁻¹, between 100 and 3200 trichomes L⁻¹, and greater than 3200 trichomes L⁻¹, respectively. Percentages of observations in each region are used to apportion N₂ fixation rates. Data are taken from Westberry *et al.* [2005], N = 184.

given here is representative of *Trichodesmium* at any given time, we can estimate the area occupied by subbloom populations and their resulting N_2 fixation rates, given the satellite-derived bloom estimates. For this case, we apply a more moderate nonbloom areal rate of N_2 fixation equal to $200 \mu\text{mol N m}^{-2} \text{d}^{-1}$ which gives annual nonbloom *Trichodesmium* N_2 fixation in the tropical and subtropical oceans $\sim 20 \text{ Tg N yr}^{-1}$. Obviously, this result is sensitive to the areal rate applied, but this value is reasonable on the basis of a compilation of measurements made by Capone *et al.* [2005]. In a very rough sense, this is in line with previous investigations. Estimates of global N_2 fixation based on biological rate measurements are $\sim 80 \text{ Tg N yr}^{-1}$ and it is thought that $\sim 40\text{--}60\%$ of this amount is directly attributable to nonbloom *Trichodesmium* [Capone *et al.*, 1997; Capone and Carpenter, 1999].

[31] In early work, Carpenter and Capone [1992] showed that inclusion of N_2 fixation by *Trichodesmium* blooms doubled ($2\times$) then present-day global N_2 fixation estimates. For lack of improved estimates, this same relationship has been applied in more recent estimates as well [see Gruber and Sarmiento, 1997]. Using a much more accurate method of accounting, the bloom results presented here somewhat support this logic, but go even further. Owing to the intensity of N_2 fixation within blooms, we find that although somewhat limited in space and time, *Trichodesmium* blooms account for a majority of the annual biological N_2 fixation. Our estimates of nonbloom background N_2 fixation are $\sim 20 \text{ Tg N yr}^{-1}$, while the bloom results add an additional 42 Tg N yr^{-1} .

5. Summary

[32] Blooms of *Trichodesmium* spp. are shown to be a widespread, yet infrequent phenomena of the tropical ocean. This much was suggested from decades worth of shipboard observation. However, vast areas of the ocean remain undersampled in space and/or time, and the remote sensing approach used here is an excellent compliment able to fill some of the spatial/temporal gaps. The region of semi-persistent blooms in the equatorial Pacific is a good example, as very few expeditions have traversed this portion of ocean, much less sought to observe *Trichodesmium* ecology. The overall impact of these blooms on N cycling in the ocean is significant, and on regional scales their role may be much more important. The magnitude of N_2 fixation estimated here shows that an accounting for *Trichodesmium* blooms must be included in determinations of the global N budget. In our estimation it is difficult to say whether this inclusion leads to a more or less balanced budget due to the large degrees of uncertainty in the various sources and sinks [e.g., Codispoti *et al.*, 2001; Gruber, 2004]. Estimates of total oceanic N_2 fixation differ greatly from investigation to investigation depending on approach and details of methodology (see Karl *et al.* [2002] for review). Denitrification estimates suffer from similar constraints. Further, the idea that these blooms, and nitrogen fixation in general, could be occurring in regions with strong denitrification is an enticing future research topic and warrants further investigation. Unraveling this potential

coupling may have significant effects on future estimates of the oceanic N budget.

[33] **Acknowledgments.** The authors would like to thank Ajit Subramaniam, Norm Nelson, Stephane Maritorena, Natalie Mahowald, Tony Michaels and many others for helpful discussions. This work would not have been possible without the many years worth of data collection by Doug Capone, Ed Carpenter, and others. Support was provided by NSF and NASA for both T. K. W. and D. A. S.

References

- Altabet, M. A., D. W. Murray, and W. L. Prell (1999), Climatically linked oscillations in Arabian Sea denitrification over the past 1 m.y.: Implications for the marine N cycle, *Paleoceanography*, *14*, 732–743.
- Banzon, V. F., R. E. Evans, H. R. Gordon, and R. M. Chomko (2004), SeaWiFS observations of the Arabian Sea southwest monsoon bloom for the year 2000, *Deep Sea Res., Part II*, *51*(1–3), 189–208.
- Behrenfeld, M. J., et al. (2001), Biospheric primary production during an ENSO transition, *Science*, *291*, 2594–2597.
- Borstad, G. A., J. F. A. Gower, and E. J. Carpenter (1992), Development of algorithms for remote sensing of *Trichodesmium* blooms, in *Marine Pelagic Cyanobacteria: Trichodesmium and Other Diazotrophs*, edited by E. J. Carpenter and D. G. Capone, pp. 193–210, Springer, New York.
- Brandes, J. A., and A. H. Devol (2002), A global marine-fixed nitrogen isotopic budget: Implications for Holocene nitrogen cycling, *Global Biogeochem. Cycles*, *16*(4), 1120, doi:10.1029/2001GB001856.
- Brandes, J. A., A. H. Devol, T. Yoshinari, D. A. Jayakumar, and S. W. A. Naqvi (1998), Isotopic composition of nitrate in the central Arabian Sea and eastern tropical North Pacific: A tracer for mixing and nitrogen cycles, *Limnol. Oceanogr.*, *43*(7), 1680–1689.
- Broecker, W. S., and G. M. Henderson (1998), The sequence of events surrounding Termination II and their implication for the cause of glacial-interglacial CO_2 changes, *Paleoceanography*, *13*, 352–364.
- Brown, C. W., and J. A. Yoder (1994), Coccolithophorid blooms in the global ocean, *J. Geophys. Res.*, *99*(4), 7467–7482.
- Capone, D. G., and E. J. Carpenter (1992), Nitrogen fixation in *Trichodesmium* blooms, in *Marine Pelagic Cyanobacteria: Trichodesmium and Other Diazotrophs*, edited by E. J. Carpenter, D. G. Capone, and J. Reuter, pp. 211–217, Springer, New York.
- Capone, D. G., and E. J. Carpenter (1999), Nitrogen fixation by marine cyanobacteria: Historical and global perspectives, *Bull. Inst. Oceanogr. Monaco*, *19*, 235–256.
- Capone, D. G., J. Zehr, H. Paerl, B. Bergman, and E. J. Carpenter (1997), *Trichodesmium*: A globally significant marine cyanobacterium, *Science*, *276*, 1221–1229.
- Capone, D. G., et al. (1998), An extensive bloom of the N_2 -fixing cyanobacterium *Trichodesmium erythraeum* in the central Arabian Sea, *Mar. Ecol. Prog. Ser.*, *172*, 281–292.
- Capone, D. G., et al. (2005), Nitrogen fixation by *Trichodesmium* spp.: An important source of new nitrogen to the tropical and subtropical North Atlantic Ocean, *Global Biogeochem. Cycles*, *19*, GB2024, doi:10.1029/2004GB002331.
- Carpenter, E. J. (1983), Nitrogen fixation by marine Oscillatoria (*Trichodesmium*) in the world's oceans, in *Nitrogen in the Marine Environment*, edited by E. J. Carpenter and D. G. Capone, pp. 65–104, Elsevier, New York.
- Carpenter, E. J., and D. G. Capone (1992), Significance of *Trichodesmium* blooms in the marine nitrogen cycle, in *Marine Pelagic Cyanobacteria: Trichodesmium and Other Diazotrophs*, edited by E. J. Carpenter, D. G. Capone, and J. Reuter, pp. 211–217, Springer, New York.
- Carpenter, E. J., and K. Romans (1991), Major role of the cyanobacterium *Trichodesmium* in nutrient cycling in the North Atlantic Ocean, *Science*, *254*, 1356–1358.
- Carpenter, E. J., H. R. Harvey, B. Fry, and D. G. Capone (1997), Biogeochemical tracers of the marine cyanobacterium *Trichodesmium*, *Deep Sea Res., Part I*, *44*(1), 27–38.
- Carpenter, E. J., A. Subramaniam, and D. G. Capone (2004), Biomass and primary productivity of the cyanobacterium *Trichodesmium* spp. in the tropical N. Atlantic Ocean, *Deep Sea Res., Part I*, *51*(2), 173–203.
- Codispoti, L. A., J. A. Brandes, J. P. Christensen, A. H. Devol, S. W. A. Naqvi, H. W. Paerl, and T. Yoshinari (2001), The oceanic fixed nitrogen and nitrous oxide budgets: Moving targets as we enter the anthropocene?, *Sci. Mar.*, *65*, suppl. 2, 85–105.
- Coles, V. J., C. Wilson, and R. R. Hood (2004), Remote sensing of new production fueled by nitrogen fixation, *Geophys. Res. Lett.*, *31*, L06301, doi:10.1029/2003GL019018.

- Conkright, M. E., H. E. Garcia, T. D. O'Brien, R. A. Locamini, T. P. Boyer, C. Stephens, and J. I. Antonov (2002), *World Ocean Atlas 2001*, vol. 4, *Nutrients*, edited by S. Levitus, *NOAA Atlas NESDIS 52*, Natl. Oceanic and Atmos. Admin., Silver Spring, Md.
- Deuser, W. (1975), Reducing environments, in *Chemical Oceanography*, edited by J. P. Riley and G. S. Skirrow, pp. 1–37, Elsevier, New York.
- Deutsch, C., N. Gruber, R. M. Key, J. L. Sarmiento, and A. Ganachaud (2001), Denitrification and N₂ fixation in the Pacific Ocean, *Global Biogeochem. Cycles*, *15*, 483–506.
- Doney, S. C. (1999), Major challenges confronting marine biogeochemical modeling, *Global Biogeochem. Cycles*, *13*, 705–714.
- Dupouy, C. (1992), Discoloured waters in the Melanesian archipelago (New Caledonia and Vanuatu): The value of the Nimbus-7 Coastal Zone Colour Scanner observations, in *Marine Pelagic Cyanobacteria: Trichodesmium and Other Diazotrophs*, edited by E. J. Carpenter, D. G. Capone, and J. Rueter, pp. 177–191, Springer, New York.
- Falkowski, P. G. (1997), Evolution of the nitrogen cycle and its influence on biological sequestration of CO₂ in the oceans, *Nature*, *387*, 272–273.
- Fiedler, P. C. (2002), The annual cycle and biological effects of the Costa Rica Dome, *Deep Sea Res., Part I*, *49*(22), 321–338.
- Ganeshram, R. S., T. F. Pederson, S. E. Calvert, G. W. McNeill, and M. R. Fontugne (2000), Glacial-interglacial variability in denitrification in the world's oceans: Causes and consequences, *Paleoceanography*, *15*, 361–376.
- Gruber, N. (2004), The dynamics of the marine N cycle and its influence on atmospheric CO₂ variation, in *Carbon Climate Interactions*, edited by M. Follows and T. Oguz, pp. 1–48, John Wiley, Hoboken, N. J.
- Gruber, N., and J. Sarmiento (1997), Global patterns of marine nitrogen fixation and denitrification, *Global Biogeochem. Cycles*, *11*, 235–266.
- Gruber, N., and J. L. Sarmiento (2002), Biogeochemical/physical interactions in elemental cycles, in *The Sea: Biological-Physical Interactions in the Oceans*, vol. 12, edited by A. R. Robinson, J. J. McCarthy, and B. J. Rothschild, pp. 337–399, John Wiley, Hoboken, N. J.
- Hansell, D. A., N. R. Bates, and D. B. Olson (2004), Excess nitrate and nitrogen fixation in the North Atlantic Ocean, *Mar. Chem.*, *84*, 243–265.
- Hood, R. R., N. R. Bates, D. G. Capone, and D. B. Olson (2001), Modeling the effect of nitrogen fixation on carbon and nitrogen fluxes at BATS, *Deep Sea Res., Part II*, *48*(8–9), 1609–1648.
- Hood, R. R., V. J. Coles, and D. G. Capone (2004), Modeling the distribution of *Trichodesmium* and nitrogen fixation in the Atlantic Ocean, *J. Geophys. Res.*, *109*, C06006, doi:10.1029/2002JC001753.
- Karl, D. M., R. Letelier, L. Tupas, J. Dore, J. Christian, and D. Hebel (1997), The role of nitrogen fixation in biogeochemical cycling in the subtropical North Pacific Ocean, *Nature*, *388*, 533–538.
- Karl, D., et al. (2002), Dinitrogen fixation in the world's oceans, *Biogeochemistry*, *57–58*, 47–98.
- Maritorena, S., D. A. Siegel, and A. R. Peterson (2002), Optimization of a semi-analytical ocean color model for global-scale applications, *Appl. Opt.*, *41*(15), 2705–2714.
- McElroy, M. B. (1983), Marine biological controls on atmospheric CO₂ climate, *Nature*, *302*, 328–329.
- Michaels, A. F., D. Olson, J. L. Sarmiento, J. W. Ammerman, K. Fanning, A. H. Knap, F. Lipschultz, and J. M. Prospero (1996), Inputs, losses and transformations of nitrogen and phosphorus in the pelagic North Atlantic Ocean, *Biogeochemistry*, *35*, 181–226.
- Michaels, A. F., D. M. Karl, and D. G. Capone (2001), Elemental stoichiometry, new production, and nitrogen fixation, *Oceanography*, *14*(4), 68–77.
- Montoya, J. P., M. Voss, P. Kahler, and D. G. Capone (1996), A simple, high-precision, high-sensitivity tracer assay for N₂ fixation, *Appl. Environ. Microbiol.*, *62*(3), 986–993.
- Montoya, J. P., C. M. Holl, J. P. Zehr, A. Hansen, T. A. Villareal, and D. G. Capone (2004), High rates of N₂ fixation by unicellular diazotrophs in the oligotrophic Pacific Ocean, *Nature*, *430*, 1027–1032.
- Moore, J. K., S. C. Doney, D. M. Glover, and I. Y. Fung (2002), Iron cycling and nutrient-limitation patterns in surface waters of the world ocean, *Deep Sea Res., Part II*, *49*(1–3), 463–507.
- O'Reilly, J. E., S. Maritorena, B. G. Mitchell, D. A. Siegel, K. L. Carder, S. A. Garver, M. Kahru, and C. McClain (1998), Ocean color chlorophyll algorithms for SeaWiFS, *J. Geophys. Res.*, *103*(C11), 24,937–24,953.
- Saji, N. H., and T. Yamagata (2002), Structure of SST and surface wind variability during Indian Ocean dipole mode events: COADS observations, *J. Clim.*, *16*(16), 2735–2751.
- Saji, N. H., B. N. Goswami, P. N. Vinayachandran, and T. Yamagata (1999), A dipole mode in the tropical Indian Ocean, *Nature*, *401*, 360–363.
- Sigman, D. M., J. Granger, P. J. DiFiore, M. M. Lehmann, R. Ho, G. Cane, and A. van Geen (2005), Coupled nitrogen and oxygen isotope measurements of nitrate along the eastern North Pacific margin, *Global Biogeochem. Cycles*, *19*, GB4022, doi:10.1029/2005GB002458.
- Soille, P. (2003), *Morphological Image Analysis: Principles and Applications*, 2nd ed., Springer, New York.
- Subramaniam, A., E. J. Carpenter, D. Karentz, and P. G. Falkowski (1999), Bio-optical properties of the marine diazotrophic cyanobacteria *Trichodesmium* spp.: I. Absorption and photosynthetic action spectra, *Limnol. Oceanogr.*, *44*(3), 608–617.
- Subramaniam, A., C. W. Brown, R. R. Hood, E. J. Carpenter, and D. G. Capone (2002), Detecting *Trichodesmium* blooms in SeaWiFS imagery, *Deep Sea Res., Part II*, *49*(1–3), 107–121.
- Westberry, T. K., D. A. Siegel, and A. Subramaniam (2005), An improved bio-optical algorithm for the remote sensing of *Trichodesmium* spp. blooms, *J. Geophys. Res.*, *110*, C06012, doi:10.1029/2004JC002517.
- Xie, S. P., H. Xu, W. S. Kessler, and M. Nonaka (2005), Air-sea interaction of the eastern Pacific Warm Pool: Gap winds, thermocline dome, and atmospheric convection, *Clim. J.*, *18*(1), 5–20.
- Zehr, J. P., J. B. Waterbury, P. J. Turner, J. P. Montoya, E. Omeregic, G. F. Steward, A. Hansen, and D. M. Karl (2001), Unicellular cyanobacteria fix N₂ in the subtropical North Pacific Ocean, *Nature*, *412*, 635–638.

D. A. Siegel, Institute for Computational Earth System Science, University of California, Santa Barbara, CA 93106, USA.

T. K. Westberry, Department of Botany and Plant Pathology, Oregon State University, 2082 Cordley Hall, Corvallis, OR 97331, USA. (westbert@science.oregonstate.edu)